NEUTRINO OSCILLATIONS AND STERILE NEUTRINO
*C. Giunti**

INFN, Sezione di Torino, Torino, Italy

We review the status of three-neutrino mixing and the results of global analyses of short-baseline neutrino oscillation data in $3+1$, $3+2$, and $3+1+1$ neutrino mixing schemes.

PACS: 14.60.Pq

INTRODUCTION

Neutrino oscillations have been measured with high accuracy in solar, atmospheric and long-baseline neutrino oscillation experiments. Hence, we know without doubt that neutrinos are massive and mixed particles (see [1]). In this short review we discuss the status of the standard three-neutrino mixing paradigm (Sec. 1) and the indications in favor of the existence of additional sterile neutrinos given by anomalies found in some short-baseline neutrino oscillation experiments (Sec. 2).

1. THREE-NEUTRINO MIXING

Solar neutrino experiments (Homestake [2], GALLEX/GNO [3], SAGE [4], Super-Kamiokande [5], SNO [6], Borexino [7]) measured $\nu_e \to \nu_\mu, \nu_\tau$ oscillations generated by the solar squared-mass difference $\Delta m^2_{\text{sol}} \simeq 7 \cdot 10^{-5}$ eV^2 and a mixing angle $\sin^2 \vartheta_{\text{sol}} \simeq 0.3$. The KamLAND experiment [8] confirmed these oscillations by observing the disappearance of reactor $\bar{\nu}_e$ with average energy $\langle E \rangle \simeq 4$ MeV at the average distance $\langle L \rangle \simeq 180$ km.

Atmospheric neutrino experiments (Kamiokande [9], IMB [10], Super-Kamiokande [11], Soudan-2 [12], MACRO [13], MINOS [14]) measured ν_μ and $\bar{\nu}_\mu$ disappearance through oscillations generated by the atmospheric squared-mass difference $\Delta m^2_{\text{atm}} \simeq 2.3 \cdot 10^{-3}$ eV^2 and a mixing angle $\sin^2 \vartheta_{\text{atm}} \simeq 0.5$. The K2K [15] and MINOS [16] long-baseline experiments confirmed these oscillations by observing the disappearance of accelerator ν_μ with $\langle E \rangle \simeq 1.3$ GeV and 3 GeV at distances $L \simeq 250$ km and 730 km, respectively.

---

*E-mail: giunti@to.infn.it

The Super-Kamiokande atmospheric neutrino data indicate that the disappearance of $\overset{(-)}{\nu}_\mu$ is likely due to $\overset{(-)}{\nu}_\mu \to \overset{(-)}{\nu}_\tau$ transitions with a statistical significance of 3.8σ [17]. This oscillation channel is confirmed at 3.4σ by the observation of three $\nu_\mu \to \nu_\tau$ events in the OPERA long-baseline accelerator experiment [18] in which the detector was exposed to the CNGS (CERN–Gran Sasso) beam with $\langle E \rangle \simeq 13$ GeV at $L \simeq 730$ km.

The two independent solar and atmospheric Δm^2's are nicely accommodated in the standard framework of three-neutrino mixing in which the left-handed components of the three active flavor neutrino fields ν_e, ν_μ, ν_τ are superpositions of three massive neutrino fields ν_1, ν_2, ν_3 with masses m_1, m_2, m_3:

$$\nu_{\alpha L} = \sum_{k=1}^{3} U_{\alpha k} \nu_{kL} \qquad (\alpha = e, \mu, \tau). \tag{1}$$

The unitary mixing matrix can be written in the standard parameterization in terms of three mixing angles ϑ_{12}, ϑ_{23}, ϑ_{13} and a CP-violating phase* δ:

$$U = \begin{pmatrix} c_{12}c_{13} & s_{12}c_{13} & s_{13}\,\mathrm{e}^{-i\delta} \\ -s_{12}c_{23} - c_{12}s_{23}s_{13}\,\mathrm{e}^{i\delta} & c_{12}c_{23} - s_{12}s_{23}s_{13}\,\mathrm{e}^{i\delta} & s_{23}c_{13} \\ s_{12}s_{23} - c_{12}c_{23}s_{13}\,\mathrm{e}^{i\delta} & -c_{12}s_{23} - s_{12}c_{23}s_{13}\,\mathrm{e}^{i\delta} & c_{23}c_{13} \end{pmatrix}, \tag{2}$$

where $c_{ab} \equiv \cos\vartheta_{ab}$ and $s_{ab} \equiv \sin\vartheta_{ab}$. It is convenient to choose the numbers of the massive neutrinos in order to have

$$\Delta m_{\mathrm{sol}}^2 = \Delta m_{21}^2 \ll \Delta m_{\mathrm{atm}}^2 = \frac{1}{2}\left|\Delta m_{31}^2 + \Delta m_{32}^2\right|, \tag{3}$$

with $\Delta m_{kj}^2 = m_k^2 - m_j^2$. Then, there are two possible hierarchies for the neutrino masses: the normal hierarchy (NH) with $m_1 < m_2 < m_3$ and the inverted hierarchy (IH) with $m_3 < m_1 < m_2$.

With the conventions in Eqs. (2) and (3), we have $\vartheta_{\mathrm{sol}} = \vartheta_{12}$ and $\vartheta_{\mathrm{atm}} = \vartheta_{23}$. Moreover, the mixing angle ϑ_{13} generates $\overset{(-)}{\nu}_e$ disappearance and $\overset{(-)}{\nu}_\mu \to \overset{(-)}{\nu}_e$ transitions driven by $\Delta m_{\mathrm{atm}}^2$, which can be observed in long-baseline neutrino oscillation experiments.

In 2011, the T2K experiment reported the first indication of long-baseline $\nu_\mu \to \nu_e$ transitions [19], followed by the MINOS experiment [20]. Recently, the T2K Collaboration reported a convincing 7.5σ observation of $\nu_\mu \to \nu_e$ transitions through the measurement of 28 ν_e events with an expected background of (4.92 ± 0.55) events [21].

---

*For simplicity, we do not consider the two Majorana CP-violating phases which contribute to neutrino mixing if massive neutrinos are Majorana particles, because they do not affect neutrino oscillations (see [1]).

On the other hand, the most precise measurement of the value of ϑ_{13} comes from the measurement of $\bar{\nu}_e$ disappearance in the Daya Bay reactor experiment [22], which has been confirmed by the data of the RENO [23] and Double Chooz [24] reactor experiments:

$$\sin^2 2\vartheta_{13} = 0.090^{+0.008}_{-0.009} \quad [25]. \tag{4}$$

Hence, we have a robust evidence of a nonzero value of ϑ_{13}, which is very important, because the measured value of ϑ_{13} opens promising perspectives for the observation of CP violation in the lepton sector and matter effects in long-baseline oscillation experiments, which could allow one to distinguish the normal and inverted neutrino mass spectra (see [26]).

Table 1. **Best fit (b.f.) values of the neutrino mixing parameters obtained in the global analysis of neutrino oscillation data presented in [27] in the framework of three-neutrino mixing with the two spectrum types (s.t.): normal spectrum (NS) and inverted spectrum (IS). The relative uncertainty (r.u.) has been obtained from the 3σ range divided by 6**

Parameter	s.t.	b.f.	1σ range	2σ range	3σ range	r.u., %
$\Delta m^2_{\mathrm{sol}}$, 10^{-5} eV^2		7.54	7.32–7.80	7.15–8.00	6.99–8.18	3
$\sin^2 \vartheta_{12}$, 10^{-1}		3.08	2.91–3.25	2.75–3.42	2.59–3.59	5
$\Delta m^2_{\mathrm{atm}}$, 10^{-3} eV^2	NS	2.44	2.38–2.52	2.30–2.59	2.22–2.66	3
	IS	2.40	2.33–2.47	2.25–2.54	2.17–2.61	3
$\sin^2 \vartheta_{23}$, 10^{-1}	NS	4.25	3.98–4.54	3.76–5.06	3.57–6.41	11
	IS	4.37	4.08–6.10	3.84–6.37	3.63–6.59	11
$\sin^2 \vartheta_{13}$, 10^{-2}	NS	2.34	2.16–2.56	1.97–2.76	1.77–2.97	9
	IS	2.39	2.18–2.60	1.98–2.80	1.78–3.00	9

The three-neutrino mixing parameters can be determined with good precision with a global fit of neutrino oscillation data. In Table 1 we report the results of the latest global fit presented in [27], which agree, within the uncertainties, with the NuFIT-v1.2 [28] update of the global analysis presented in [29]. One can see that all the oscillation parameters are determined with precision between about 3 and 11%. The largest uncertainty is that of ϑ_{23}, which is known to be close to maximal ($\pi/4$), but it is not known if it is smaller or larger than $\pi/4$. For the Dirac CP-violating phase δ, there is an indication in favor of $\delta \approx 3\pi/2$, which would give maximal CP violation, but at 3σ all the values of δ are allowed, including the CP-conserving values $\delta = 0, \pi$.

2. BEYOND THREE-NEUTRINO MIXING: STERILE NEUTRINOS

The completeness of the three-neutrino mixing paradigm has been challenged by the following indications in favor of short-baseline neutrino oscillations, which

require the existence of at least one additional squared-mass difference, $\Delta m^2_{\mathrm{sbl}}$, which is much larger than $\Delta m^2_{\mathrm{sol}}$ and $\Delta m^2_{\mathrm{atm}}$:

1. The reactor antineutrino anomaly [30], which is a deficit of the rate of $\bar{\nu}_e$ observed in several short-baseline reactor neutrino experiments in comparison with that expected from a new calculation of the reactor neutrino fluxes [31, 32]. The statistical significance is about 2.8σ.

2. The Gallium neutrino anomaly [33–37], consisting in a short-baseline disappearance of ν_e measured in the Gallium radioactive source experiments GALLEX [38] and SAGE [39] with a statistical significance of about 2.9σ.

3. The LSND experiment, in which a signal of short-baseline $\bar{\nu}_\mu \to \bar{\nu}_e$ oscillations has been observed with a statistical significance of about 3.8σ [40, 41].

In this review, we consider $3 + 1$ [42–45], $3 + 2$ [46–49], and $3 + 1 + 1$ [50–53] neutrino mixing schemes in which there are one or two additional massive neutrinos at the eV scale and the masses of the three standard massive neutrinos are much smaller. Since from the LEP measurement of the invisible width of the Z boson we know that there are only three active neutrinos (see [1]), in the flavor basis the additional massive neutrinos correspond to sterile neutrinos [54], which do not have standard weak interactions.

The possible existence of sterile neutrinos is very interesting, because they are new particles which could give us precious information on the physics beyond the Standard Model (see [55, 56]). The existence of light sterile neutrinos is also very important for astrophysics (see [57]) and cosmology (see [58, 59]). In the $3 + 1$ scheme, the effective probability of $\overset{(-)}{\nu}_\alpha \to \overset{(-)}{\nu}_\beta$ transitions in short-baseline experiments has the two-neutrino-like form

$$P_{\overset{(-)}{\nu}_\alpha \to \overset{(-)}{\nu}_\beta} = \delta_{\alpha\beta} - 4|U_{\alpha 4}|^2 \left(\delta_{\alpha\beta} - |U_{\beta 4}|^2\right) \sin^2\left(\frac{\Delta m^2_{41} L}{4E}\right), \tag{5}$$

where U is the mixing matrix, L is the source-detector distance, E is the neutrino energy and $\Delta m^2_{41} = m^2_4 - m^2_1 = \Delta m^2_{\mathrm{sbl}} \sim 1$ eV^2. The electron and muon neutrino and antineutrino appearance and disappearance in short-baseline experiments depend on $|U_{e4}|^2$ and $|U_{\mu 4}|^2$, which determine the amplitude $\sin^2 2\vartheta_{e\mu} = 4|U_{e4}|^2|U_{\mu 4}|^2$ of $\overset{(-)}{\nu}_\mu \to \overset{(-)}{\nu}_e$ transitions, the amplitude $\sin^2 2\vartheta_{ee} = 4|U_{e4}|^2(1 - |U_{e4}|^2)$ of $\overset{(-)}{\nu}_e$ disappearance, and the amplitude $\sin^2 2\vartheta_{\mu\mu} = 4|U_{\mu 4}|^2(1 - |U_{\mu 4}|^2)$ of $\overset{(-)}{\nu}_\mu$ disappearance.

Since the oscillation probabilities of neutrinos and antineutrinos are related by a complex conjugation of the elements of the mixing matrix (see [1]), the effective probabilities of short-baseline $\nu_\mu \to \nu_e$ and $\bar{\nu}_\mu \to \bar{\nu}_e$ transitions are equal. Hence, the $3 + 1$ scheme cannot explain a possible CP-violating difference of $\nu_\mu \to \nu_e$ and $\bar{\nu}_\mu \to \bar{\nu}_e$ transitions in short-baseline experiments. In order to allow this possibility, one must consider a $3 + 2$ scheme, in which, there

are four additional effective mixing parameters in short-baseline experiments: $\Delta m_{51}^2 \geqslant \Delta m_{41}^2$, $|U_{e5}|^2$, $|U_{\mu5}|^2$, and $\eta = \arg\left[U_{e4}^* U_{\mu4} U_{e5} U_{\mu5}^*\right]$ (see [60, 61]). Since this complex phase appears with different signs in the effective $3+2$ probabilities of short-baseline $\nu_\mu \to \nu_e$ and $\bar{\nu}_\mu \to \bar{\nu}_e$ transitions, it can generate measurable CP violations.

A puzzling feature of the $3+2$ scheme is that it needs the existence of two sterile neutrinos with masses at the eV scale. We think that it may be considered as more plausible that sterile neutrinos have a hierarchy of masses. Hence, it is interesting to consider also the $3+1+1$ scheme [50–53], in which m_5 is much heavier than 1 eV and the oscillations due to Δm_{51}^2 are averaged. Hence, in the analysis of short-baseline data in the $3+1+1$ scheme there is one effective parameter less than in the $3+2$ scheme (Δm_{51}^2), but CP violations generated by η are observable.

Global fits of short-baseline neutrino oscillation data have been presented recently in [62, 63]. These analyses take into account the final results of the MiniBooNE experiment, which was made in order to check the LSND signal with about one order of magnitude larger distance (L) and energy (E), but the same order of magnitude for the ratio L/E from which neutrino oscillations depend. Unfortunately, the results of the MiniBooNE experiment are ambiguous, because the LSND signal was not seen in neutrino mode [64], and the signal observed in 2010 [65] with the first half of the antineutrino data was not observed in the second half of the data [66]. Moreover, the MiniBooNE data in both neutrino and antineutrino modes show an excess in the low-energy bins which is widely considered to be anomalous because it is at odds with neutrino oscillations [67, 68]*.

In the following we summarize the results of the analysis of short-baseline data, presented in [63], of the following three groups of experiments:

(a) The $\overset{\scriptscriptstyle(-)}{\nu}_\mu \to \overset{\scriptscriptstyle(-)}{\nu}_e$ appearance data of the LSND [41], MiniBooNE [66], BNL-E776 [71], KARMEN [72], NOMAD [73], ICARUS [74], and OPERA [75] experiments.

(b) The $\overset{\scriptscriptstyle(-)}{\nu}_e$ disappearance data described in [37], which take into account the reactor [30–32] and Gallium [33–36, 76] anomalies.

(c) The constraints on $\overset{\scriptscriptstyle(-)}{\nu}_\mu$ disappearance obtained from the data of the CDHSW experiment [77], from the analysis [48] of the data of atmospheric neutrino oscillation experiments**, from the analysis [67] of the MINOS neutral-current data [80], and from the analysis of the SciBooNE-MiniBooNE neutrino [81] and antineutrino [82] data.

---

*The interesting possibility of reconciling the low-energy anomalous data with neutrino oscillations through energy reconstruction effects proposed in [69, 70] still needs a detailed study.

**The IceCube data, which could give a marginal contribution [78, 79], have not been considered because the analysis is too complicated and subject to large uncertainties.

Table 2. **Results of the fit of short-baseline data [63] taking into account all MiniBooNE data (LOW), only the MiniBooNE data above 475 MeV (HIG),without MiniBooNE data (noMB) and without LSND data (noLSND) in the $3+1$, $3+2$, and $3+1+1$ schemes. The first three lines give the minimum χ^2 ($\chi^2_{\min}$), the number of degrees of freedom (NDF), and the goodness-of-fit (GoF). The following five lines give the quantities relevant for the appearance–disappearance (APP–DIS) parameter goodness-of-fit (PG) [83]. The last three lines give the difference between the χ^2 without short-baseline oscillations and $\chi^2_{\min}$ ($\Delta\chi^2_{\mathrm{NO}}$), the corresponding difference of number of degrees of freedom (NDF$_{\mathrm{NO}}$) and the resulting number of σ's ($n\sigma_{\mathrm{NO}}$) for which the absence of oscillations is disfavored**

Parameter	$3+1$ LOW	$3+1$ HIG	$3+1$ noMB	$3+1$ noLSND	$3+2$ LOW	$3+2$ HIG	$3+1+1$ LOW	$3+1,+1$ HIG
$\chi^2_{\min}$	291.7	261. 8	236.1	278.4	284.4	256.4	289.8	259.0
NDF	256	250	218	252	252	246	253	247
GoF, %	6	29	19	12	8	31	6	29
$(\chi^2_{\min})_{\mathrm{APP}}$	99.3	77.0	50.9	91.8	87.7	69.8	94.8	75.5
$(\chi^2_{\min})_{\mathrm{DIS}}$	180.1	180.1	180.1	180.1	179.1	179.1	180.1	180.1
$\Delta\chi^2_{\mathrm{PG}}$	12.7	4.8	5.1	6.4	17.7	7.5	14.9	3.4
NDF$_{\mathrm{PG}}$	2	2	2	2	4	4	3	3
GoF$_{\mathrm{PG}}$, %	0.2	9	8	4	0.1	11	0.2	34
$\Delta\chi^2_{\mathrm{NO}}$	47.5	46.2	47.1	8.3	54.8	51.6	49.4	49.1
NDF$_{\mathrm{NO}}$	3	3	3	3	7	7	6	6
$n\sigma_{\mathrm{NO}}$	6.3σ	6.2σ	6.3σ	2.1σ	6.0σ	5.8σ	5.8σ	5.8σ

Table 2 summarizes the statistical results obtained in [63] from global fits of the data above in the $3+1$, $3+2$, and $3+1+1$ schemes. In the LOW fits, all the MiniBooNE data are considered, including the anomalous low-energy bins, which are omitted in the HIG fits. There is also a $3+1$-noMB fit without MiniBooNE data and a $3+1$-noLSND fit without LSND data.

From Table 2, one can see that in all fits which include the LSND data the absence of short-baseline oscillations is disfavored by about 6σ, because the improvement of the χ^2 with short-baseline oscillations is much larger than the number of oscillation parameters.

In all the $3+1$, $3+2$, and $3+1+1$ schemes the goodness-of-fit in the LOW analysis is significantly worse than that in the HIG analysis and the appearance–disappearance parameter goodness-of-fit is much worse. This result confirms the fact that the MiniBooNE low-energy anomaly is incompatible with neutrino oscillations, because it would require a small value of Δm^2_{41} and a large value of $\sin^2 2\vartheta_{e\mu}$ [67,68], which are excluded by the data of other experiments (see [63]

for further details)*. Note that the appearance–disappearance tension in the $3+2$-LOW fit is even worse than that in the $3+1$-LOW fit, since the $\Delta\chi^2_{\mathrm{PG}}$ is so much larger that it cannot be compensated by the additional degrees of freedom (this behavior has been explained in [84]). Therefore, we think that it is very likely that the MiniBooNE low-energy anomaly has an explanation which is different from neutrino oscillations and the HIG fits are more reliable than the LOW fits.

The $3+2$ mixing scheme, was considered to be interesting in 2010 when the MiniBooNE neutrino [64] and antineutrino [65] data showed a CP-violating tension. Unfortunately, this tension reduced considerably in the final MiniBooNE data [66], and from Table 2 one can see that there is little improvement of the $3+2$-HIG fit with respect to the $3+1$-HIG fit, in spite of the four additional parameters and the additional possibility of CP violation. Moreover, since the p-value obtained by restricting the $3+2$ scheme to $3+1$ disfavors the $3+1$ scheme only at 1.2σ [63], we think that considering the larger complexity of the $3+2$ scheme is not justified by the data**.

The results of the $3+1+1$-HIG fit presented in Table 2 show that the appearance–disappearance parameter goodness-of-fit is remarkably good, with a $\Delta\chi^2_{\mathrm{PG}}$ that is smaller than those in the $3+1$-HIG and $3+2$-HIG fits. However, the $\chi^2_{\min}$ in the $3+1+1$-HIG is only slightly smaller than that in the $3+1$-HIG fit and the p-value obtained by restricting the $3+1+1$ scheme to $3+1$ disfavors the $3+1$ scheme only at 0.8σ [63]. Therefore, there is no compelling reason to prefer the more complex $3+1+1$ to the simpler $3+1$ scheme.

The Figure shows the allowed regions in the $\sin^2 2\vartheta_{e\mu}$–Δm^2_{41}, $\sin^2 2\vartheta_{ee}$–Δm^2_{41}, and $\sin^2 2\vartheta_{\mu\mu}$–$\Delta m^2_{41}$ planes obtained in the $3+1$-HIG fit of [63]. These regions are relevant, respectively, for $\overset{(-)}{\nu}_\mu \to \overset{(-)}{\nu}_e$ appearance, $\overset{(-)}{\nu}_e$ disappearance, and $\overset{(-)}{\nu}_\mu$ disappearance searches. The corresponding marginal-allowed intervals of the oscillation parameters are given in Table 3. The Figure shows also the region allowed by $\overset{(-)}{\nu}_\mu \to \overset{(-)}{\nu}_e$ appearance data and the constraints from $\overset{(-)}{\nu}_e$ disappearance and $\overset{(-)}{\nu}_\mu$ disappearance data. One can see that the combined disappearance constraint in the $\sin^2 2\vartheta_{e\mu}$–Δm^2_{41} plane excludes a large part of the region allowed by $\overset{(-)}{\nu}_\mu \to \overset{(-)}{\nu}_e$ appearance data, leading to the well-known appearance–disappearance tension [61, 62, 67, 68, 84–87] quantified by the parameter goodness-of-fit in Table 2.

It is interesting to investigate what is the impact of the MiniBooNE experiment on the global analysis of short-baseline neutrino oscillation data. With this

---

*One could fit the three anomalous MiniBooNE low-energy bins in a $3+2$ scheme [61] by considering the appearance data without the ICARUS [74] and OPERA [75] constraints, but the corresponding relatively large transition probabilities are excluded by the disappearance data.

**See, however, the somewhat different conclusions reached in [62].
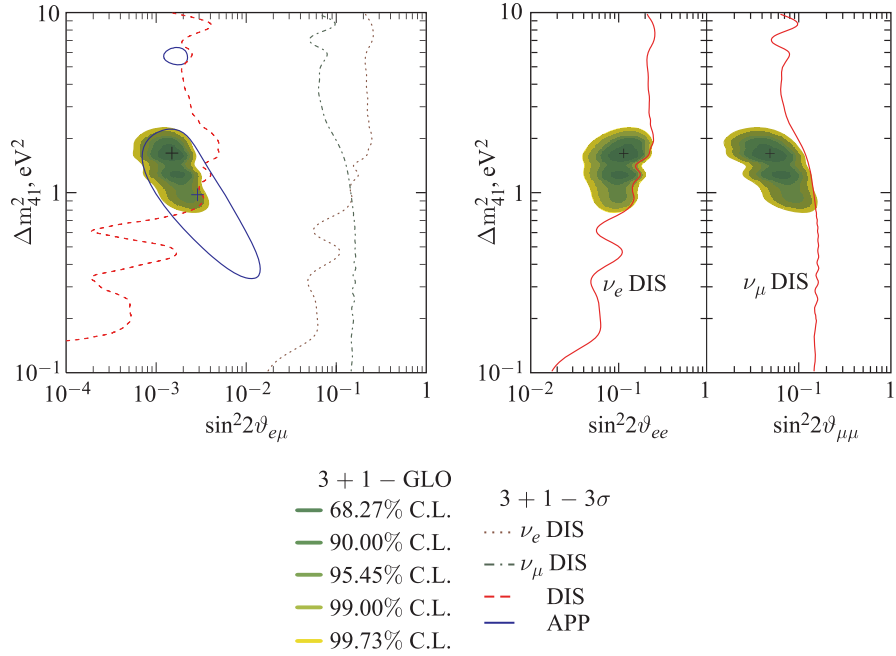
Color online. Allowed regions in the $\sin^2 2\vartheta_{e\mu} - \Delta m_{41}^2$, $\sin^2 2\vartheta_{ee} - \Delta m_{41}^2$, and $\sin^2 2\vartheta_{\mu\mu} - \Delta m_{41}^2$ planes obtained in the global (GLO) $3+1$-HIG fit [63] of short-baseline neutrino oscillation data compared with the 3σ allowed regions obtained from $\overset{(-)}{\nu}_\mu \to \overset{(-)}{\nu}_e$ short-baseline appearance data (APP) and the 3σ constraints obtained from $\overset{(-)}{\nu}_e$ short-baseline disappearance data (ν_e DIS), $\overset{(-)}{\nu}_\mu$ short-baseline disappearance data (ν_μ DIS) and the combined short-baseline disappearance data (DIS). The best-fit points of the GLO and APP fits are indicated by crosses

Table 3. **Marginal allowed intervals of the oscillation parameters obtained in the global $3+1$-HIG fit of short-baseline neutrino oscillation data [63]**

C.L., %	Δm_{41}^2, eV^2	$\sin^2 2\vartheta_{e\mu}$	$\sin^2 2\vartheta_{ee}$	$\sin^2 2\vartheta_{\mu\mu}$
68.27	1.55–1.72	0.0012–0.0018	0.089–0.15	0.036–0.065
90.00	1.19–1.91	0.001–0.0022	0.072–0.17	0.03–0.085
95.00	1.15–1.97	0.00093–0.0023	0.066–0.18	0.028–0.095
95.45	1.14–1.97	0.00091–0.0024	0.065–0.18	0.027–0.095
99.00	0.87–2.09	0.00078–0.003	0.054–0.2	0.022–0.12
99.73	0.82–2.19	0.00066–0.0034	0.047–0.22	0.019–0.14

aim, the authors of [63] performed two additional $3+1$ fits: a $3+1$-noMB fit without MiniBooNE data and a $3+1$-noLSND fit without LSND data. From Table 2, one can see that the results of the $3+1$-noMB fit are similar to those of

the $3+1$-HIG fit and the exclusion of the case of no-oscillations remains at the level of 6σ. On the other hand, in the $3+1$-noLSND fit, without LSND data, the exclusion of the case of no-oscillations drops dramatically to 2.1σ. In fact, in this case the main indication in favor of short-baseline oscillations is given by the reactor and gallium anomalies which have a similar statistical significance (see Introduction). Therefore, it is clear that the LSND experiment is still crucial for the indication in favor of short-baseline $\bar{\nu}_\mu \to \bar{\nu}_e$ transitions and the MiniBooNE experiment has been rather inconclusive.

In conclusion, the results of the global fit of short-baseline neutrino oscillation data presented in [63] show that the data can be explained by $3+1$ neutrino mixing and this simplest scheme beyond three-neutrino mixing cannot be rejected in favor of the more complex $3+2$ and $3+1+1$ schemes. The low-energy MiniBooNE anomaly cannot be explained by neutrino oscillations in any of these schemes. Moreover, the crucial indication in favor of short-baseline $\bar{\nu}_\mu \to \bar{\nu}_e$ appearance is still given by the old LSND data, and the MiniBooNE experiment has been inconclusive. Hence new better experiments are needed in order to check this signal [88–92].

REFERENCES

1. *Giunti C., Kim C. W.* Fundamentals of Neutrino Physics and Astrophysics. Oxford, UK: Oxford Univ. Press, 2007.

2. *Cleveland B. T. et al.* Measurement of the Solar Electron Neutrino Flux with the Homestake Chlorine Detector // Astrophys. J. 1998. V. 496. P. 505.

3. *Altmann M. et al. (GNO Collab.).* Complete Results for Five Years of GNO Solar Neutrino Observations // Phys. Lett. B. 2005. V. 616. P. 174.

4. *Abdurashitov J. N. et al. (SAGE Collab.)* // J. Exp. Theor. Phys. 2002. V. 95. P. 181.

5. *Abe K. et al. (Super-Kamiokande Collab.).* Solar Neutrino Results in Super-Kamiokande-III // Phys. Rev. D. 2011. V. 83. P. 052010.

6. *Aharmim B. et al. (SNO Collab.).* Combined Analysis of All Three Phases of Solar Neutrino Data from the Sudbury Neutrino Observatory // Phys. Rev. C. 2013. V. 88. P. 025501.

7. *Bellini G. et al. (Borexino Collab.).* Final Results of Borexino Phase-I on Low Energy Solar Neutrino Spectroscopy. arXiv:1308.0443.

8. *Gando A. et al. (KamLAND Collab.).* Reactor On-Off Antineutrino Measurement with KamLAND // Phys. Rev. D. 2013. V. 88. P. 033001.

9. *Fukuda Y. et al. (Kamiokande Collab.).* Atmospheric Muon–Neutrino / Electron–Neutrino Ratio in the MultiGeV Energy Range // Phys. Lett. B. 1994. V. 335. P. 237.

10. *Becker-Szendy R. et al. (IMB Collab.).* The Electron–Neutrino and Muon–Neutrino Content of the Atmospheric Flux // Phys. Rev. D. 1992. V. 46. P. 3720.

11. *Fukuda Y. et al. (Super-Kamiokande Collab.).* Evidence for Oscillation of Atmospheric Neutrinos // Phys. Rev. Lett. 1998. V. 81. P. 1562.

12. *Sanchez M. et al. (Soudan Collab.).* Measurement of the L/E Distributions of Atmospheric Neutrinos in Soudan 2 and Their Interpretation as Neutrino Oscillations // Phys. Rev. D. 2003. V. 68. P. 113004.

13. *Ambrosio M. et al. (MACRO Collab.).* Atmospheric Neutrino Oscillations from Upward through Going Muon Multiple Scattering in MACRO // Phys. Lett. B. 2003. V. 566. P. 35.

14. *Adamson P. et al. (MINOS Collab.).* Measurements of Atmospheric Neutrinos and Antineutrinos in the MINOS Far Detector // Phys. Rev. D. 2012. V. 86. P. 052007.

15. *Ahn M. H. et al. (K2K Collab.).* Measurement of Neutrino Oscillation by the K2K Experiment // Phys. Rev. D. 2006. V. 74. P. 072003.

16. *Adamson P. et al. (MINOS Collab.).* An Improved Measurement of Muon Antineutrino Disappearance in MINOS // Phys. Rev. Lett. 2012. V. 108. P. 191801.

17. *Abe K. et al. (Super-Kamiokande Collab.).* A Measurement of the Appearance of Atmospheric Tau Neutrinos by Super-Kamiokande // Phys. Rev. Lett. 2013. V. 110. P. 181802.

18. *Agafonova N. et al. (OPERA Collab.).* Evidence for $\nu_\mu \to \nu_\tau$ Appearance in the CNGS Neutrino Beam with the OPERA Experiment // Phys. Rev. D. 2014. V. 89. P. 051102.

19. *Abe K. et al. (T2K Collab.).* Indication of Electron Neutrino Appearance from an Accelerator-Produced Off-Axis Muon Neutrino Beam // Phys. Rev. Lett. 2011. V. 107. P. 041801.

20. *Adamson P. et al. (MINOS Collab.).* Improved Search for Muon–Neutrino to Electron–Neutrino Oscillations in MINOS // Phys. Rev. Lett. 2011. V. 107. P. 181802.

21. *Abe K. et al. (T2K Collab.).* Observation of Electron Neutrino Appearance in a Muon Neutrino Beam // Phys. Rev. Lett. 2014. V. 112. P. 061802.

22. *An F. P. et al. (Daya Bay Collab.).* Observation of Electron–Antineutrino Disappearance at Daya Bay // Phys. Rev. Lett. 2012. V. 108. P. 171803.

23. *Kim S.-B. et al. (RENO Collab.).* Observation of Reactor Electron Antineutrino Disappearance in the RENO Experiment // Ibid. P. 191802.

24. *Abe Y. et al. (Double Chooz Collab.).* First Measurement of θ_{13} from Delayed Neutron Capture on Hydrogen in the Double Chooz Experiment // Phys. Lett. B. 2013. V. 723. P. 66.

25. *An F. et al. (Daya Bay Collab.).* Spectral Measurement of Electron Antineutrino Oscillation Amplitude and Frequency at Daya Bay // Phys. Rev. Lett. 2014. V. 112. P. 061801.

26. *Mezzetto M., Schwetz T.* θ_{13}: Phenomenology, Present Status and Prospect // J. Phys. G. 2010. V. 37. P. 103001.

27. *Capozzi F. et al.* Status of Three-Neutrino Oscillation Parameters, Circa 2013 // Phys. Rev. D. 2014. V. 89. 093018.

28. NuFIT. http://www.nu-fit.org/.

29. *Gonzalez-Garcia M. et al.* Global Fit to Three-Neutrino Mixing: Critical Look at Present Precision // JHEP. 2012. V. 12. P. 123.

30. *Mention G. et al.* The Reactor Antineutrino Anomaly // Phys. Rev. D. 2011. V. 83. P. 073006.

31. *Mueller Th. A. et al.* Improved Predictions of Reactor Antineutrino Spectra // Phys. Rev. C. 2011. V. 83. P. 054615.

32. *Huber P.* On the Determination of Antineutrino Spectra from Nuclear Reactors // Ibid. P. 024617.

33. *Abdurashitov J. N. et al. (SAGE Collab.).* Measurement of the Solar Neutrino Capture Rate with Gallium Metal // Phys. Rev. C. 2006. V. 73. P. 045805.

34. *Laveder M.* Unbound Neutrino Roadmaps // Nucl. Phys. Proc. Suppl. 2007. V. 168. P. 344; Workshop on Neutrino Oscillation Physics (NOW 2006), Otranto, Lecce, Italy, Sept. 9–16, 2006.

35. *Giunti C., Laveder M.* Short-Baseline Active-Sterile Neutrino Oscillations? // Mod. Phys. Lett. A. 2007. V. 22. P. 2499.

36. *Giunti C., Laveder M.* Statistical Significance of the Gallium Anomaly // Phys. Rev. C. 2011. V. 83. P. 065504.

37. *Giunti C. et al.* Update of Short-Baseline Electron Neutrino and Antineutrino Disappearance // Phys. Rev. D. 2012. V. 86. P. 113014.

38. *Kaether F. et al.* Reanalysis of the GALLEX Solar Neutrino Flux and Source Experiments // Phys. Lett. B. 2010. V. 685. P. 47.

39. *Abdurashitov J. N. et al. (SAGE Collab.).* Measurement of the Solar Neutrino Capture Rate with Gallium Metal. III: Results for the 2002–2007 Data-Taking Period // Phys. Rev. C. 2009. V. 80. P. 015807.

40. *Athanassopoulos C. et al. (LSND Collab.).* Candidate Events in a Search for Antimuon–Neutrino → Antielectron–Neutrino Oscillations // Phys. Rev. Lett. 1995. V. 75. P. 2650.

41. *Aguilar A. et al. (LSND Collab.).* Evidence for Neutrino Oscillations from the Observation of Antineutrino (Electron) Appearance in an Antineutrino (Muon) Beam // Phys. Rev. D. 2001. V. 64. P. 112007.

42. *Okada N., Yasuda O.* A Sterile Neutrino Scenario Constrained by Experiments and Cosmology // Intern. J. Mod. Phys. A. 1997. V. 12. P. 3669.

43. *Bilenky S. M., Giunti C., Grimus W.* Neutrino Mass Spectrum from the Results of Neutrino Oscillation Experiments // Eur. Phys. J. C. 1998. V. 1. P. 247.

44. *Bilenky S. M. et al.* Four Neutrino Mass Spectra and the Super-Kamiokande Atmospheric Up-Down Asymmetry // Phys. Rev. D. 1999. V. 60. P. 073007.

45. *Maltoni M. et al.* // New J. Phys. 2004. V. 6. P. 122.

46. *Sorel M., Conrad J., Shaevitz M.* A Combined Analysis of Short-Baseline Neutrino Experiments in the $(3+1)$ and $(3+2)$ Sterile Neutrino Oscillation Hypotheses // Phys. Rev. D. 2004. V. 70. P. 073004.

47. *Karagiorgi G. et al.* Leptonic CP-Violation Studies at MiniBooNE in the $(3+2)$ Sterile Neutrino Oscillation Hypothesis // Phys. Rev. D. 2007. V. 75. P. 013011.

48. *Maltoni M., Schwetz T.* Sterile Neutrino Oscillations after First MiniBooNE Results // Ibid. P. 093005.

49. *Karagiorgi G. et al.* Viability of Delta m^2 1-eV^2 Sterile Neutrino Mixing Models in Light of MiniBooNE Electron-Neutrino and Antineutrino Data from the Booster and NuMI Beamlines // Phys. Rev. D. 2009. V. 80. P. 073001.

50. *Nelson A. E.* Effects of CP Violation from Neutral Heavy Fermions on Neutrino Oscillations, and the LSND/MiniBooNE Anomalies // Phys. Rev. D. 2011. V. 84. P. 053001.

51. *Fan J., Langacker P.* Light Sterile Neutrinos and Short Baseline Neutrino Oscillation Anomalies // JHEP. 2012. V. 04. P. 083.

52. *Kuflik E., McDermott S. D., Zurek K. M.* Neutrino Phenomenology in a $3+1+1$ Framework // Phys. Rev. D. 2012. V. 86. P. 033015.

53. *Huang J., Nelson A. E.* MeV Dark Matter in the $3+1+1$ Model // Phys. Rev. D. 2013. V. 88. P. 033016.

54. *Pontecorvo B.* Neutrino Experiments and the Problem of Conservation of Leptonic Charge // Sov. Phys. JETP. 1968. V. 26. P. 984.

55. *Volkas R. R.* Introduction to Sterile Neutrinos // Prog. Part. Nucl. Phys. 2002. V. 48. P. 161.

56. *Mohapatra R. N., Smirnov A. Y.* Neutrino Mass and New Physics // Ann. Rev. Nucl. Part. Sci. 2006. V. 56. P. 569.

57. *Diaferio A., Angus G. W.* The Acceleration Scale, Modified Newtonian Dynamics, and Sterile Neutrinos. arXiv:1206.6231.

58. *Riemer-Sorensen S., Parkinson D., Davis T. M.* What Is Half a Neutrino? Reviewing Cosmological Constraints on Neutrinos and Dark Radiation. arXiv:1301.7102.

59. *Archidiacono M. et al.* // Adv. High Energy Phys. 2013. V. 2013. P. 191047.

60. *Gonzalez-Garcia M. C., Maltoni M.* Phenomenology with Massive Neutrinos // Phys. Rep. 2008. V. 460. P. 1.

61. *Conrad J. et al.* // Adv. High Energy Phys. 2013. V. 2013. P. 163897.

62. *Kopp J. et al.* Sterile Neutrino Oscillations: The Global Picture // JHEP. 2013. V. 1305. P. 050.

63. *Giunti C. et al.* Pragmatic View of Short-Baseline Neutrino Oscillations // Phys. Rev. D. 2013. V. 88. P. 073008.

64. *Aguilar-Arevalo A. A. et al. (MiniBooNE Collab.).* Unexplained Excess of Electron-Like Events From a 1-GeV Neutrino Beam // Phys. Rev. Lett. 2009. V. 102. P. 101802.

65. *Aguilar-Arevalo A. A. et al. (MiniBooNE Collab.).* Event Excess in the MiniBooNE Search for $\bar{\nu}_\mu \to \bar{\nu}_e$ Oscillations // Phys. Rev. Lett. 2010. V. 105. P. 181801.

66. *Aguilar-Arevalo A. et al. (MiniBooNE Collab.).* Improved Search for $\bar{\nu}_\mu \to \bar{\nu}_e$ Oscillations in the MiniBooNE Experiment // Phys. Rev. Lett. 2013. V. 110. P. 161801.

67. *Giunti C., Laveder M.* Status of $3+1$ Neutrino Mixing // Phys. Rev. D. 2011. V. 84. P. 093006.

68. *Giunti C., Laveder M.* Implications of $3+1$ Short-Baseline Neutrino Oscillations // Phys. Lett. B. 2011. V. 706. P. 200.

69. *Martini M., Ericson M., Chanfray G.* Neutrino Energy Reconstruction Problems and Neutrino Oscillations // Phys. Rev. D. 2012. V. 85. P. 093012.

70. *Martini M., Ericson M., Chanfray G.* Energy Reconstruction Effects in Neutrino Oscillation Experiments and Implications for the Analysis // Phys. Rev. D. 2013. V. 87. P. 013009.

71. *Borodovsky L. et al. (BNL-E776 Collab.).* Search for Muon–Neutrino Oscillations Muon–Neutrino → Electron–Neutrino (Antimuon–Neutrino → Antielectron–Neutrino in a Wide Band Neutrino Beam // Phys. Rev. Lett. 1992. V. 68. P. 274.

72. *Armbruster B. et al. (KARMEN Collab.).* Upper Limits for Neutrino Oscillations Muon–Antineutrino → Electron–Antineutrino from Muon Decay at Rest // Phys. Rev. D. 2002. V. 65. P. 112001.

73. *Astier P. et al. (NOMAD Collab.).* Search for $\nu(\mu) \to \nu(e)$ Oscillations in the NOMAD Experiment // Phys. Lett. B. 2003. V. 570. P. 19.

74. *Antonello M. et al. (ICARUS Collab.).* Search for Anomalies in the ν_e Appearance from a ν_μ Beam // Eur. Phys. J. C. 2013. V. 73. P. 2599.

75. *Agafonova N. et al. (OPERA Collab.).* Search for $\nu_\mu \to \nu_e$ Oscillations with the OPERA Experiment in the CNGS Beam // JHEP. 2013. V. 1307. P. 004.

76. *Acero M. A., Giunti C., Laveder M.* Limits on $\nu(e)$ and $\bar{\nu}(e)$ Disappearance from Gallium and Reactor Experiments // Phys. Rev. D. 2008. V. 78. P. 073009.

77. *Dydak F. et al. (CDHSW Collab.).* A Search for Muon–Neutrino Oscillations in the Δm^2 Range 0.3-eV^2 to 90-eV^2 // Phys. Lett. B. 1984. V. 134. P. 281.

78. *Esmaili A., Halzen F., Peres O. L. G.* Probing the Stability of Superheavy Dark Matter Particles with High-Energy Neutrinos // JCAP. 2012. V. 1211. P. 041.

79. *Esmaili A., Smirnov A. Y.* Restricting the LSND and MiniBooNE Sterile Neutrinos with the IceCube Atmospheric Neutrino Data // JHEP. 2013. V. 1312. P. 014.

80. *Adamson P. et al. (MINOS Collab.).* Active to Sterile Neutrino Mixing Limits from Neutral-Current Interactions in MINOS // Phys. Rev. Lett. 2011. V. 107. P. 011802.

81. *Mahn K. B. M. et al. (SciBooNE-MiniBooNE Collab.).* Dual Baseline Search for Muon Neutrino Disappearance at $0.5 \text{ eV}^2 < \Delta m^2 < 40 \text{ eV}^2$ // Phys. Rev. D. 2012. V. 85. P. 032007.

82. *Cheng G. et al. (SciBooNE-MiniBooNE Collab.).* Dual Baseline Search for Muon Antineutrino Disappearance at $0.1 \text{ eV}^2 < \Delta m^2 < 100 \text{ eV}^2$ // Ibid. P. 052009.

83. *Maltoni M., Schwetz T.* Testing the Statistical Compatibility of Independent Data Sets // Phys. Rev. D. 2003. V. 68. P. 033020.

84. *Archidiacono M. et al.* Sterile Neutrinos: Cosmology Versus Short-Baseline Experiments // Phys. Rev. D. 2013. V. 87. P. 125034.

85. *Kopp J., Maltoni M., Schwetz T.* Are There Sterile Neutrinos at the eV Scale? // Phys. Rev. Lett. 2011. V. 107. P. 091801.

86. *Giunti C., Laveder M.* $3+1$ and $3+2$ Sterile Neutrino Fits // Phys. Rev. D. 2011. V. 84. P. 073008.

87. *Archidiacono M. et al.* Testing $3+1$ and $3+2$ Neutrino Mass Models with Cosmology and Short-Baseline Experiments // Phys. Rev. D. 2012. V. 86. P. 065028.

88. *Abazajian K. N. et al.* Light Sterile Neutrinos: A White Paper. arXiv:1204.5379.

89. *Rubbia C. et al.* Sterile Neutrinos: The Necessity for a 5 Sigma Definitive Clarification. arXiv:1304.2047.

90. *Elnimr M. et al. (OscSNS Collab.).* The OscSNS White Paper. arXiv:1307.7097.

91. *Delahaye J-P. et al.* Enabling Intensity and Energy Frontier Science with a Muon Accelerator Facility in the U.S.: A White Paper Submitted to the 2013 U.S. Community Summer Study of the Division of Particles and Fields of the Amer. arXiv:1308.0494.

92. *Adey D. et al. (nuSTORM Collab.).* nuSTORM — Neutrinos from STORed Muons: Proposal to the Fermilab PAC. arXiv:1308.6822.